Nigerian Journal of Physics (NJP)
ISSN online: 3027-0936
ISSN print: 1595-0611
DOI: https://doi.org/10.62292/njp.v35(S).2026.786
Volume 35(S), November 2026

Assessment of Groundwater Potential and Aquifer Protective Capacity in Maraban Lapai, Niger State, Nigeria, using Electrical Resistivity Sounding and Dar-Zarrouk Parameters

***Hadiza H. Ndanusa[1], Halidu I.[2], Abdulwahid K. Aweda[2], Maryam Mohammed[1]**

[1]Department of Physics, Faculty of Physical Sciences, Ibrahim Badamasi Babangida University, Lapai, Niger State, Nigeria
[2]Department of Geology, Faculty of Physical Sciences, Ibrahim Badamasi Babangida University, Lapai, Niger State, Nigeria

*Corresponding Author's Email: hadizandanusa@ibbu.edu.ng

Keywords:
Vertical Electrical Sounding; Dar-Zarrouk Parameters; Basement Complex; Aquifer Protective Capacity; Lapai

Submitted: 9/10/2026
Accepted: 17/11/2026
Published: 18/11/2026

ABSTRACT

Groundwater in the crystalline basement complex of central Nigeria occurs mainly in the weathered regolith and fracture networks overlying fresh basement. This study applied Schlumberger vertical electrical sounding (VES) at twenty stations around Maraban Lapai, Niger State, to delineate the geoelectric framework and to make a preliminary, resistivity-based assessment of groundwater prospectivity and aquifer protective capacity using Dar-Zarrouk parameters. Half-spacing AB/2 was expanded from 1 to 100 m, and the curves were interpreted by partial curve-matching and iterative inversion (WinResist) to obtain three- and four-layer models. Eleven stations are H-type, three A-type, two HA-type, two KH-type, one HK-type and one K-type. The inferred weathered-basement horizon has its base at depths of 2.0–37.4 m, with resistivity of 6.2–3,712.5 Ω·m. On resistivity and modelled thickness alone, five stations (VES 1, 9, 14, 18 and 19) are classed as very good and four (VES 6, 13, 17 and 20) as good geoelectric prospects; seven stations, including VES 9, 18 and 19, had RMS misfit above 15%, so their models are provisional. The longitudinal conductance of the cover above the inferred aquifer ranged from below 0.001 to 0.186 mho, placing seventeen stations in the poor and three in the weak protective-capacity class, which suggests little electrical evidence of natural protection, although the cover layers are thin and poorly resolved. These are geophysical inferences, subject to the non-uniqueness of resistivity interpretation, and have not been verified against borehole, water-table or pumping-test data. These are preliminary targets, not confirmed productive borehole sites.

INTRODUCTION

Access to safe, reliable drinking water continues to rank among the most pressing developmental challenges facing rural and peri-urban communities across sub-Saharan Africa, and Nigeria's central basement complex belt is no exception. Rapid, largely unplanned settlement growth in towns such as Lapai, the headquarters of Lapai Local Government Area in Niger State, has repeatedly outpaced the moribund water infrastructure, leaving many households dependent on shallow hand-dug wells that are vulnerable to contamination and seasonal failure. Addressing this gap sustainably requires that new boreholes be sited on the basis of proven subsurface hydrogeological conditions rather than convenience or anecdote, and that the resulting aquifers be assessed not only for yield but for their natural vulnerability to surface-derived contamination (Osumeje et al., 2024).

The Precambrian crystalline rocks that underlie central Nigeria chiefly migmatitic gneisses, granites, schists and quartzites possess negligible primary porosity and permeability (Rahaman, 1976). Groundwater in such terrain is therefore controlled entirely by secondary structures: the weathered residual overburden (regolith) and the fracture and joint systems that penetrate the underlying fresh basement (Jones & Hockey, 1964; Dada, 2006). The productivity of any borehole sunk into this environment depends on the thickness, saturation

and lateral continuity of these secondary features, none of which can be reliably inferred from surface geological mapping alone (Olayinka, 1996). Prior geophysical investigation is consequently a practical prerequisite for cost-effective borehole siting in basement complex settings.

The Schlumberger vertical electrical sounding (VES) technique remains the method of choice for hydrogeophysical reconnaissance of basement aquifers in Nigeria, owing to its low cost, operational simplicity and demonstrated reliability (Olorunfemi & Fasuyi, 1993; Olayinka & Yaramanci, 2000). By systematically expanding the current electrode spacing about a fixed sounding center, VES surveys resolve the variation of true resistivity with depth and thereby constrain layer thicknesses, depths and lithological character (Telford et al., 1990). Beyond layer identification, the derived resistivity–thickness pairs can be combined into Dar-Zarrouk parameters longitudinal conductance and transverse resistance which provide an independent, physically grounded measure of both aquifer transmissive capacity and the degree to which the overlying strata protect the aquifer from surface contamination (Henriet, 1976). This combined approach has been applied with success in different regions and geological terrains in Nigeria, including at Guyuk in the northeast (Usman Baba et al., 2026), Yola in the Upper Benue Trough (Oniku et al., 2025), and Asaba in the Niger Delta (Chukwusa et al., 2026).

These applications differ in terrain, instrumentation and interpretation, and their conclusions cannot be transferred directly to Maraban Lapai. Within Niger State, the Minna basement surveys (Obiora & Ibuot, 2018; Batagarawa & Onoduku, 2014) are the closest geological analogues, whereas the Yola and Asaba studies (Oniku et al., 2025; Chukwusa et al., 2026) were conducted in sedimentary settings, where resistivity responds to different controls than in basement regolith. The most direct precedent is the twelve-station survey of the wider Lapai basement terrain (Ndanusa et al., 2026). That survey established a regional geoelectric baseline, but it did not assess overburden protective capacity, and its station density gives limited coverage of any individual locality.

Published information on groundwater occurrence in Lapai itself is sparse. Borehole lithology compiled by Bashir et al. (2014) places the aquifer at depths of 34–40 m in the basement part of Lapai and 40–50 m in its sedimentary part. A regional compilation for Niger State classifies Lapai as a basement–sedimentary contact area, records a water level of about 6 m at Lapai, and reports that wells and boreholes in such contact areas are very deep and poor, sometimes yielding less than 0.4 l/s (Idris-Nda et al., 2015). A groundwater-quality study of 35 hand-dug wells in Lapai reports mean total coliform of 150.30 cfu/100 mL and E. coli of 65.50 cfu/100 mL, attributed to wells sited close to unlined soakaways and pit latrines, and describes the area as a transition (contact) zone with a NE–SW structural trend (Amadi et al., 2017). The twelve-station survey of Ndanusa et al. (2026) interpreted a conductive weathered-basement horizon of 11–140 Ω·m and 12–22 m thickness, with its base at 14–22.5 m depth at the H- and HA-type stations, and proposed boreholes of about 70 m. These results are compared quantitatively with the Maraban Lapai dataset in the Discussion. Borehole depth, yield and static water-level records for Maraban Lapai itself are not included in the present study.

Resistivity-derived hydrogeological parameters also have inherent limitations. Layer resistivity reflects lithology, clay content, degree of saturation and pore-water salinity together, so different combinations can produce similar values, and the interpretation of a one-dimensional sounding is not unique (the principle of equivalence). Layer thickness and depth are model-dependent, and Dar-Zarrouk protective-capacity classes describe the electrical character of the overlying cover rather than measured contaminant attenuation. The results presented here are therefore treated as preliminary targets for independent hydrogeological verification.

The contribution of this study is a locality-scale dataset of twenty soundings for Maraban Lapai, for which no geoelectric or protective-capacity dataset has previously been compiled, together with a protective-capacity analysis that the earlier Lapai survey did not include. The study was designed to: (i) establish the geoelectric stratigraphy at twenty VES stations distributed across the Maraban Lapai area; (ii) derive layered resistivity models through partial curve-matching and iterative inversion; (iii) classify each sounding curve by type and characterise the associated hydrogeological regime; (iv) construct an apparent resistivity pseudo-section to illustrate the lateral continuity of the weathered aquifer; (v) compute Dar-Zarrouk parameters at each station and evaluate the protective capacity of the cover overlying the inferred aquifer; and (vi) provide a preliminary geoelectric prospectivity classification to identify candidate targets for further investigation.

MATERIALS AND METHODS

Study Area

The study area lies within Maraban Lapai, southern Niger State, central Nigeria, along the Bida–Abuja road corridor, broadly within the coordinate range of latitudes 9°02′N to 9°04′N and longitudes 6°35′E to 6°37′E (Figure 1). Local landmarks used for station referencing include the Rugan Fulani Nomadic School, situated near the western edge of the survey area. The area falls within the North Central Basement Complex, and is underlain by Precambrian migmatite-gneiss lithologies subjected to repeated metamorphism and deformation

during the Pan-African orogeny at approximately 600 Ma (Kearey et al., 2002), producing the fracture, joint and shear-zone networks that constitute the principal secondary porosity conduits for groundwater in the area. A variably developed lateritic and sandy residual overburden, produced by long-term tropical chemical weathering, mantles the fresh basement across the survey area. The climate follows the typical West African wet–dry pattern, with a wet season from May to October and mean annual rainfall of the order of 1,100 mm; local drainage is directed broadly eastward into minor tributaries of the Gbako River, part of the River Niger catchment. Regionally, Lapai lies at the fringe of the Bida Basin and is mostly on the basement complex, within a basement–sedimentary contact zone less than 500 m wide (Idris-Nda et al., 2015). The available Figure 1 is a station-location map showing the VES positions and local geographic features; it is not a detailed geological or hydrogeological map. No verified Maraban Lapai borehole inventory, site-specific lithological logs, lineament map or hydrogeological map was available for this revision. Accordingly, the regional geological description is used as context and should not be interpreted as a substitute for locality-scale geological or hydrogeological mapping.

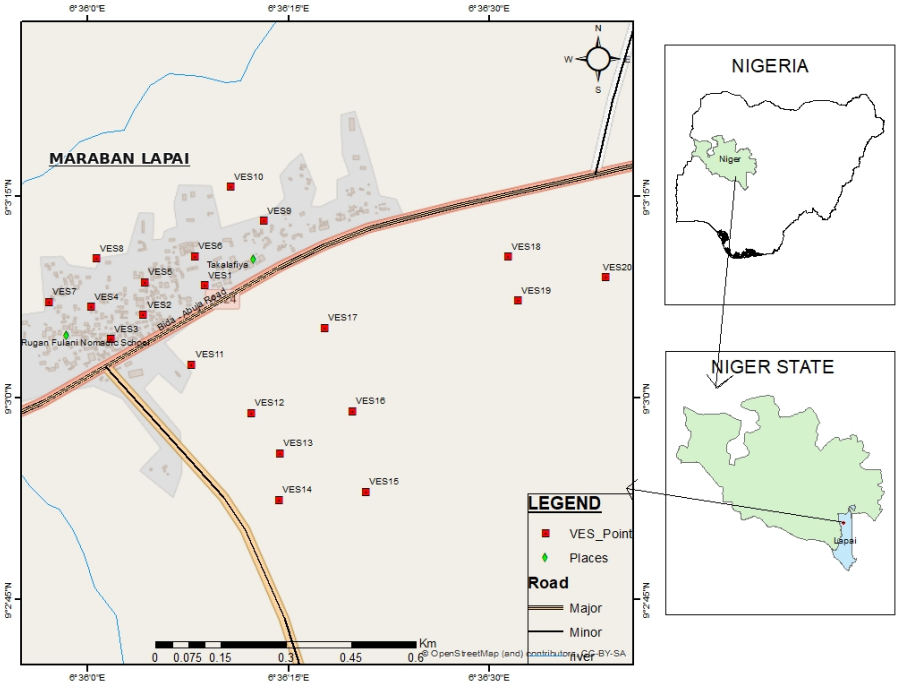


Figure 1: Location of the twenty VES stations within the study area

Field Acquisition

Twenty VES stations were distributed across accessible parts of the Maraban Lapai area to provide spatial coverage of both the built-up settlement and the more open ground around its southern and eastern margins. This was a purposive spatial arrangement rather than a statistically random sample: VES 1–11 lie within or at the margin of the built-up area, whereas VES 12–20 occupy open ground to the south and east (Figure 1). The Schlumberger electrode configuration was adopted throughout, with the current electrodes (C_1 C_2) expanded symmetrically about a fixed sounding centre and the potential electrodes (P_1 P_2) repositioned at prescribed intervals to maintain an adequate signal-to-noise ratio. Current electrode half-spacing (AB/2) was extended progressively from 1 m to 100 m at each station, with the potential electrode half-spacing (MN/2) widened in stages from 0.5 m to 15 m as required to preserve measurement sensitivity at larger spacing. For a maximum AB/2 of 100 m, the depth of investigation is a fraction of the array length (Barker, 1989), of the order of several tens of metres below ground surface; this is adequate to intersect the weathered horizon and the upper basement at most stations, but the deepest layer is only weakly constrained. A Direct Data Resistivity (DDR-2) meter was used throughout, and GPS coordinates were recorded at each station for spatial referencing.

Apparent resistivity at each measurement step was computed from the standard Schlumberger relation (Telford et al., 1990):

$$\rho_a = K \cdot \left(\frac{\Delta V}{I}\right) \qquad (1)$$

where ρ_a is the apparent resistivity, ΔV is the measured potential difference between the potential electrodes, I is the injected current and K is the Schlumberger geometric factor (Telford et al., 1990):

$$K = \frac{\pi[(AB/2)^2-(MN/2)^2]}{MN} \quad (2)$$

where AB/2 and MN/2 are the current- and potential-electrode half-spacings, respectively.

Data Processing and Inversion

Field apparent resistivity data were plotted as bilogarithmic curves of ρ_a against AB/2 and given a preliminary qualitative interpretation by partial curve-matching against standard two-layer master curves and auxiliary charts following the procedure of Orellana and Mooney (1966). These initial estimates served as starting models for computer-assisted iterative least-squares inversion in WinResist (the Windows version of RESIST; Vander Velpen, 1988; Vander Velpen & Sporry, 1993), which minimises the root-mean-square (RMS) misfit between the observed and theoretically computed apparent resistivity curves and offers a smoothing step for noisy field data. Theoretical forward-model curves were computed from the interpreted layer parameters (Koefoed, 1979) and are presented alongside the field data in Figures 2–5. Station-by-station RMS misfit is listed in Table 2 and ranged from 5.1% to 46.6%. For VES 11–20 the program reported the misfit on smoothed data, which is not strictly comparable with the unsmoothed values for VES 1–10 and may understate the misfit relative to the raw readings. Models with an RMS misfit of 15% or less are regarded here as acceptable, those between 15% and 30% (VES 2, 8, 9, 18 and 19) as marginal, and those above 30% (VES 15 and 20) as unreliable. The seven stations above 15% are marked (†) in Tables 2 and 3: their layer parameters carry wider uncertainty, and any prospectivity or protective-capacity class derived from them is treated as provisional pending verification of the field data and, where necessary, repeat measurements. Formal model-uncertainty estimates, such as equivalence ranges, are not reported here.

Curve Type Classification and Groundwater Prospectivity

Each accepted inversion model was classified according to the relative magnitudes of the interpreted true layer resistivities, following the standard basement-complex nomenclature: H-type ($\rho_1 > \rho_2 < \rho_3$), A-type ($\rho_1 < \rho_2 < \rho_3$), K-type ($\rho_1 < \rho_2 > \rho_3$) and Q-type ($\rho_1 > \rho_2 > \rho_3$) for three-layer models, with the corresponding compound types (HA, KH, HK, AK, etc.) used for four-layer models to describe two consecutive resistivity transitions (Koefoed, 1979; Telford et al., 1990). Geoelectric groundwater prospectivity (GWP) at each station was assessed from the resistivity and thickness of the weathered-basement horizon, the layer immediately overlying the fresh basement and inferred in each model to be the principal aquifer target. These are inferred quantities: the thickness used is the modelled thickness of the weathered layer, not a confirmed saturated thickness. Stations with weathered-horizon resistivity between 10 and 150 Ω·m and a modelled thickness of at least 10 m were rated very good; the same resistivity range with thickness between 3 and 10 m was rated good; resistivity below 10 Ω·m (indicative of high clay content and low permeability) or thickness below 3 m was rated moderate; and resistivity above 150 Ω·m, interpreted as a compact, poorly saturated or clay-poor horizon rather than a productive aquifer (Olorunfemi & Fasuyi, 1993), was rated poor. These thresholds are empirical and have not been calibrated against borehole records, water-table observations or pumping-test results for the study area, so the ratings are preliminary geoelectric prospectivity classes.

Dar-Zarrouk Parameters and Aquifer Protective Capacity

To complement the curve-based prospectivity assessment, Dar-Zarrouk parameters were computed from the interpreted layer resistivities and thicknesses following Maillet (1947) and Henriet (1976). Two intervals are distinguished. The total weathered overburden is the sequence of all finite-thickness layers above the fresh basement; it is used to derive the longitudinal unit conductance (S), the transverse unit resistance (T) and the related parameters below. The protective cover is defined here as only those layers lying above the top of the inferred aquifer (the weathered-basement horizon identified in Table 2), because surface-derived contaminants must pass through this cover to reach the aquifer. The aquifer horizon itself is excluded from the conductance of the cover (Sc), because its own conductance reflects transmissive rather than protective character. For a three-layer model Sc is therefore h_1 / ρ_1, and for a four-layer model it is $h_1 / \rho_1 + h_2 / \rho_2$. The parameters were computed as:

$$S = \sum_{i=1}^{n-1} \frac{h_i}{\rho_i} \quad (3)$$

$$T = \sum_{i=1}^{n-1} h_i \cdot \rho_i \quad (4)$$

summed over the i = 1 … n−1 finite-thickness layers overlying the fresh basement, where h_i and ρ_i are the thickness and true resistivity of layer i, and n is the number of layers including the basement. The conductance of the protective cover is obtained by the same summation restricted to the k layers above the top of the inferred aquifer:

$$S_c = \sum_{i=1}^{k} \frac{h_i}{\rho_i} \quad (5)$$

The total overburden thickness (H), average longitudinal resistivity (ρL), average transverse resistivity (ρT) and

coefficient of anisotropy (λ) were derived from S and T at each station:

$$H = \sum_{i=1}^{n-1} h_i \quad (6)$$

$$\rho_{\mathrm{L}} = \frac{H}{S} \quad (7)$$

$$\rho_{\mathrm{T}} = \frac{T}{H} \quad (8)$$

$$\lambda = \sqrt{\frac{\rho_{\mathrm{T}}}{\rho_{\mathrm{L}}}} \quad (9)$$

Protective capacity was classified from Sc using the empirical scheme widely applied in Nigerian basement studies, which builds on the Dar-Zarrouk concept of Henriet (1976): Sc > 10 mho = excellent, 5–10 mho = very good, 0.7–4.9 mho = good, 0.2–0.69 mho = moderate, 0.1–0.19 mho = weak and < 0.1 mho = poor (Chukwusa et al., 2026; Usman Baba et al., 2026). The class limits are empirical and have not been calibrated against measured contaminant transport at Maraban Lapai, so the classes describe the electrical character of the cover and not confirmed contaminant attenuation.

RESULTS AND DISCUSSION

Apparent Resistivity Data and Field Curve Quality

Table 1(a) and Table 1(b) present the measured apparent resistivity values for VES 1–10 and VES 11–20 respectively, at the full range of electrode spacings employed, together with the GPS coordinates of each station.

Table 1(a): Measured apparent resistivity (Ω·m) and station coordinates for VES 1–10.

AB/2 (m)	VES1	VES2	VES3	VES4	VES5	VES6	VES7	VES8	VES9	VES10
Coordinates	N09˚03' 08.38"; E6˚36'0 8.73"	N09˚03' 06.18"; E6˚36'0 4.18"	N09˚03' 04.37"; E6˚36'0 1.74"	N09˚03' 06.77"; E6˚36'0 0.28"	N09˚03' 08.62"; E6˚36'0 4.26"	N09˚03' 10.53"; E6˚36'0 8.03"	N09˚03' 07.15"; E6˚35'5 7.15"	N09˚03' 10.39"; E6˚36'0 0.65"	N09˚03' 13.17"; E6˚36'1 3.17"	N09˚03' 15.70"; E6˚36'1 0.70"
1	58	125	30	62	57	14	73	735	49	276
2	60	93	40	59	20	38	24	631	38	156
3	116	90	62	44	54	38	63	488	24	167
5	115	137	30	24	20	33	57	132	22	191
6	108	86	32	35	26	36	30	188	24	189
8	108	50	38	35	32	18	25	268	29	243
10	107	89	48	39	39	35	23	289	36	247
12	104	165	55	106	46	34	20	331	39	253
15	111	228	74	49	56	82	25	559	50	278
20	134	181	89	59	62	62	35	114	20	292
25	132	249	109	74	69	89	43	233	59	292
30	174	309	208	84	112	112	51	459	22	326
40	150	226	170	116	109	116	94	171	107	330
50	195	317	127	143	204	164	113	159	148	328
60	245	52	156	252	259	193	141	186	171	393
70	399	85	172	183	122	223	162	203	193	426
80	243	53	207	199	133	263	188	200	226	414
100	256	317	256	184	442	399	235	255	287	399

Table 1(b): Measured apparent resistivity (Ω·m) and station coordinates for VES 11–20.

AB/2 (m)	VES11	VES12	VES13	VES14	VES15	VES16	VES17	VES18	VES19	VES20
Coordinates	N9˚03'0 2.47"; E6˚36'0 7.74"	N9˚2'58 .872"; E6˚36'1 2.223"	N9˚2'55 .878"; E6˚36'1 4.368"	N09˚2'5 2.405"; E6˚36'1 4.275"	N9˚2'52 .990"; E6˚36'2 0.776"	N9˚2'58 .991"; E6˚36'1 9.775"	N9˚3'5. 192"; E6˚36' 17.70"	N9˚3'10 .509"; E6˚36'3 1.384"	N9˚3'7. 2324"; E6˚36'3 2.093"	N9˚3'8. 9608"; E6˚36'3 8.639"
1	196.4	18.93	82.12	123.19	139.47	19.42	311.92	494.89	342.21	0.779
2	120.9	15.9	28.63	19.1	34.93	18.84	147.5	130.87	359.9	31.86
3	60.6	15.67	32.4	11.62	26.29	11.9	49.5	15.39	265.25	584.16
5	52.1	24.89	28.01	42.01	12.45	13.22	19.5	12.44	66.9	222.51
6	47.2	41.55	42.7	34.81	32.57	14.59	53.9	5.6	35.93	162.84
6	60.4	34.03	54.4	21.96	15.92	6.03	27.4	4.94	55.4	195.9
8	56.4	35.60	76.2	23.73	42.53	20.76	27.7	39.56	31.65	317.46

10	292.3	55.98	77.8	24.88	38.88	91.74	27.9	7.78	24.88	163.27
10	77.2	47.70	61.3	17.67	15.31	25.3	15.3	8.41	28.86	65.37
15	92.1	82.47	83.8	24.73	30.23	38.47	31.6	10.57	97.55	72.82
20	116.3	98.96	98.9	24.74	51.95	44.53	44.5	19.78	44.52	51.95
25	136.1	116.64	116.6	50.54	58.32	54.4	62.2	19.44	89.42	89.42
30	174.1	174.09	123.6	44.92	78.62	98.2	89.9	16.84	33.69	146.01
40	210.3	130.19	170.3	60.09	771.1	50.27	170.3	30.05	21.7	385.19
40	216.6	239.24	126.1	25.96	248.9	96.9	54.9	6.47	6.46	248.69
50	235.5	281.54	163.8	81.90	568	120.07	97.2	30.71	92.14	193.16
60	232.8	245.74	181.1	90.53	593.7	133.59	111.3	51.73	58.2	248.73
70	334.8	324.7	223.2	122.75	720.4	121.75	81.17	60.88	406.8	215.87
80	327.1	345.5	252.5	132.05	122.19	173.2	159.45	66.4	52.6	306.64
80	420.4	586.2	219.9	68.55	60.7	115.2	239.28	51.73	64.67	248.73
90	326.8	552.5	494.8	148.4	98.9	177.2	197.95	82.48	239.19	208.78
100	395.4	573.3	317.3	194.3	71.65	229.2	214.9	102.37	131.03	292.48

The individual VES sounding curves for all twenty stations are presented as bilogarithmic panels in Figures 2–5, with observed field data shown as crosses/markers and the theoretical three- or four-layer forward-model curves as solid green lines, reproduced directly from the WinResist inversion output for each station.

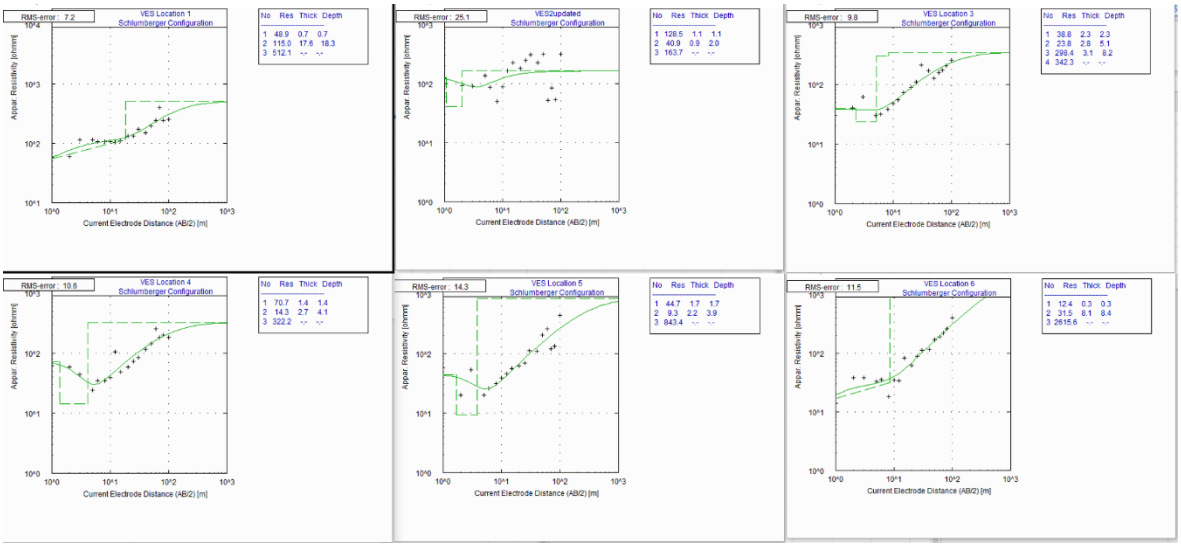


Figure 2: Schlumberger VES sounding curves and inverted layer models for stations VES 1–6.

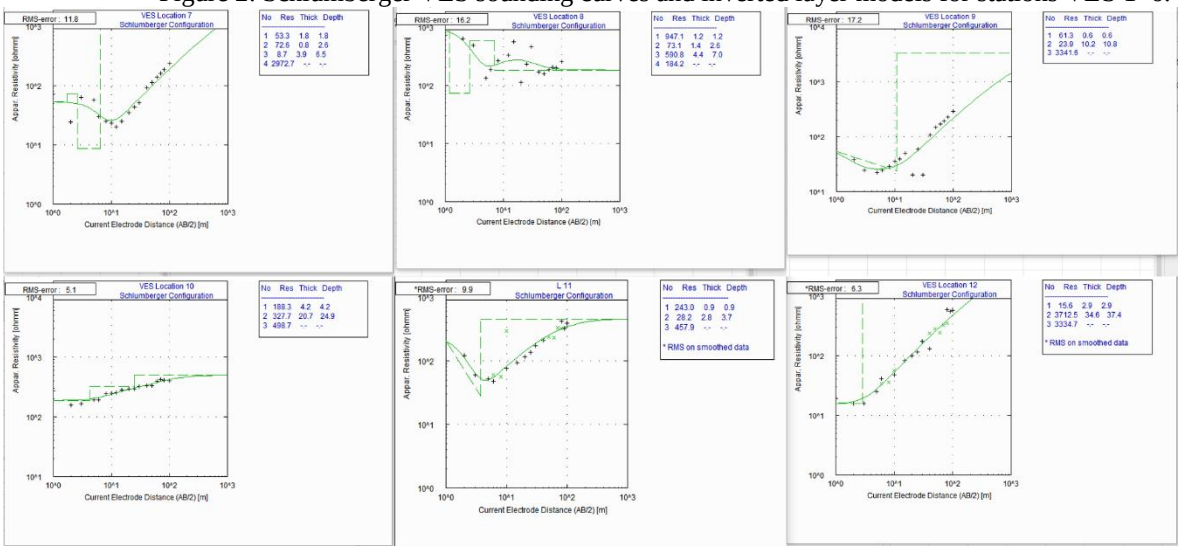


Figure 3: Schlumberger VES sounding curves and inverted layer models for stations VES 7–12. VES 7 shows the diagnostic KH-type response and VES 8 the HK-type response.

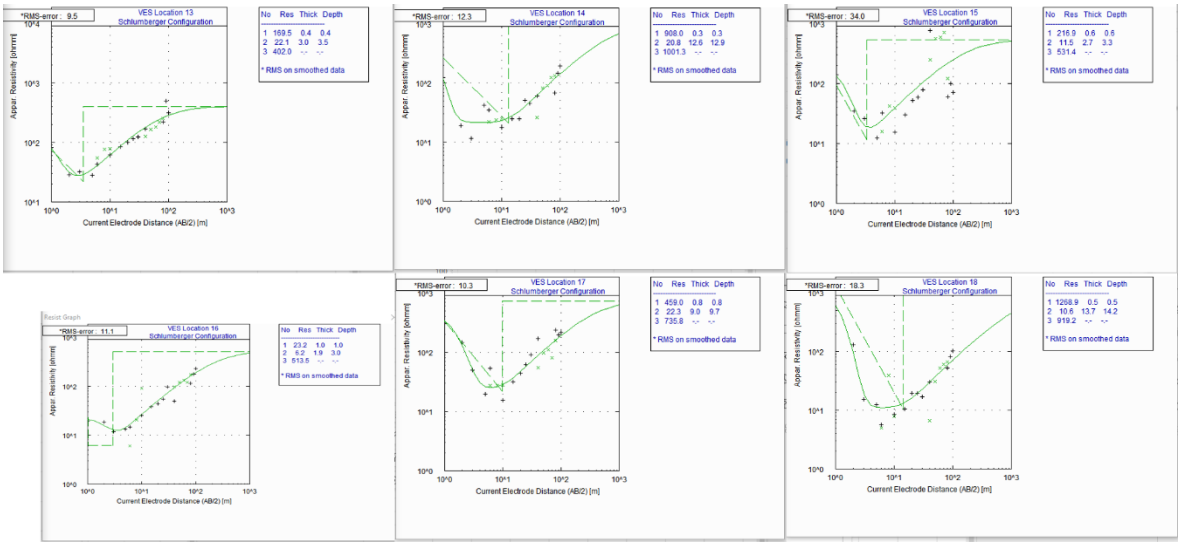


Figure 4: Schlumberger VES sounding curves and inverted layer models for stations VES 13–18.

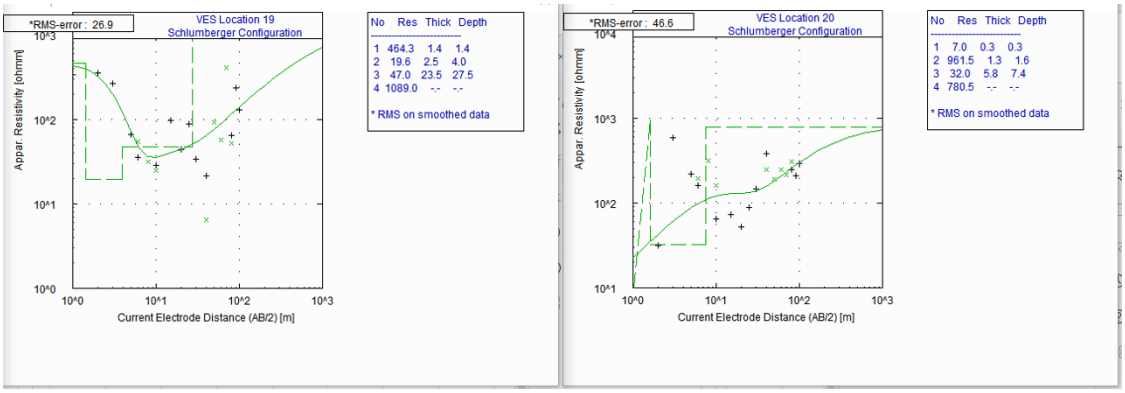


Figure 5: Schlumberger VES sounding curves and inverted layer models for stations VES 19–20 (HA-type and KH-type respectively).

Geoelectric Layer Models and Curve Classification

Of the twenty stations interpreted, eleven (VES 2, 4, 5, 9, 11, 13, 14, 15, 16, 17 and 18) yield three-layer H-type models, three (VES 1, 6 and 10) yield three-layer A-type models, two (VES 3 and 19) yield four-layer HA-type models, two (VES 7 and 20) yield four-layer KH-type models, one (VES 8) yields a four-layer HK-type model, and one (VES 12) yields a three-layer K-type model. The dominance of H-type responses is consistent with the general basement-complex pattern reported for the wider Lapai area (Ndanusa et al., 2026) and elsewhere in Niger State (Obiora & Ibuot, 2018; Batagarawa & Onoduku, 2014), in which a resistive lateritic topsoil overlies a conductive weathered zone (probably saturated) before the resistivity recovers into the fresh basement. The three A-type stations (VES 1, 6 and 10) instead show resistivity increasing progressively with depth, without an intervening conductive trough, consistent with a topsoil that grades gradually into a moderately resistive weathered zone rather than a sharply saturated one.

The four-layer stations record an additional near-surface horizon probable lateritic clay at VES 3, 8 and 19, and probable lateritic sand at VES 7 and 20 inserted between the topsoil and the weathered basement proper. At the two KH-type stations (VES 7 and VES 20) and the single HK-type station (VES 8), this intermediate horizon is markedly more resistive than both the layer above and the layer below, the diagnostic signature of a compact, poorly permeable duricrust rather than a productive aquifer (Olorunfemi & Fasuyi, 1993). The single K-type station, VES 12, shows an exceptionally resistive second layer (3,712.5 Ω·m) sandwiched between less resistive topsoil and fresh basement; although this layer is nominally the position occupied by the weathered basement elsewhere in the survey, its

resistivity is roughly two orders of magnitude higher than the weathered-zone values recorded at the H- and A-type stations, indicating a dry, compact, and effectively non-productive horizon at this location. These lithological assignments are probable interpretations based on resistivity alone; no borehole logs or geological sections were available to confirm them.

Pseudo-Section Analysis

The apparent resistivity pseudo-section (Figure 6), constructed by interpolating the measured apparent resistivity values across all twenty stations at equal assumed spacing, provides a spatially integrated view of the resistivity structure across the survey transect. A discontinuous band of lower apparent resistivity is evident at intermediate AB/2 values beneath several stations in the eastern part of the survey area (around VES 14–18), consistent with the cluster of H-type stations with thick, moderately conductive weathered zones identified above. In contrast, persistently high apparent resistivity at all depths beneath VES 8, VES 10 and VES 12 corroborates the poor-prospectivity rating assigned to these stations below.

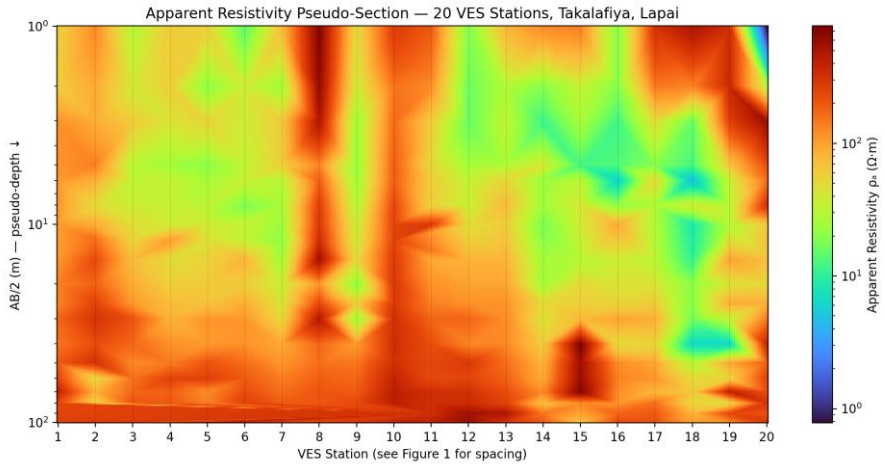


Figure 6: Apparent resistivity pseudo-section for all twenty VES stations (equal station spacing assumed). Warmer colours indicate resistive, likely dry or clay-poor horizons; cooler colours indicate more conductive, saturated horizons.

Groundwater Prospectivity Assessment

Table 2 presents the interpreted geoelectric parameters, curve classification and geoelectric groundwater prospectivity (GWP) rating for all twenty stations. The ratings are preliminary classes based on the resistivity and modelled thickness of the inferred weathered-basement horizon (see Materials and Methods) and have not been validated against hydrogeological data. Five stations (VES 1, 9, 14, 18 and 19) are rated very good, combining weathered-horizon resistivity in the 10–150 Ω·m range with a modelled thickness of at least 10 m (10.2–23.5 m). VES 19 has the greatest modelled thickness (23.5 m) and a resistivity of 47.0 Ω·m, but its RMS misfit is 26.9% (marginal), so its rating is provisional and it should not be regarded as the strongest prospect until its model has been verified; the models at VES 9 (17.2%) and VES 18 (18.3%) are also marginal, so three of the five very-good ratings are provisional. Four stations (VES 6, 13, 17 and 20) are rated good, with adequate resistivity but thinner (3.0–9.0 m) modelled sections; VES 20 has the highest misfit in the dataset (46.6%), so its rating is unreliable. Seven stations are rated moderate, either because the weathered horizon is thin (under 3 m, as at VES 2, 4, 11 and 15) or because its resistivity is below 10 Ω·m, indicating probable high clay content and reduced permeability (VES 5, 7 and 16). The remaining four stations (VES 3, 8, 10 and 12) are rated poor: at each, the horizon in the weathered-basement position is markedly resistive (298–3,713 Ω·m), consistent with a compact, dry or clay-poor horizon rather than a saturated aquifer. The largest modelled resistivities (for example 3,712.5 Ω·m at VES 12 and 3,341.6 Ω·m at VES 9) exceed the highest apparent resistivity measured at those stations (573 and 287 Ω·m, respectively), so they are extrapolated values constrained only by the shape of the curve. Fracture density, transmissivity, recharge and water-table depth were not available, so the ratings reflect electrical character only.

Table 2: Interpreted geoelectric layer parameters, curve classification and geoelectric groundwater prospectivity (GWP) rating for all twenty VES stations. ρ = true layer resistivity (topsoil → base, in layer order); h = layer thickness; D = cumulative depth to base of layer; aquifer parameters refer to the inferred weathered-basement horizon (Layer 2 for three-layer H/A/K models, Layer 3 for four-layer HA/KH/HK models), and the aquifer thickness is the modelled, not a confirmed saturated, thickness. RMS = root-mean-square misfit of the inversion; * = RMS computed by the program on smoothed data (VES 11–20), which is not strictly comparable with the unsmoothed values for VES 1–10. † = RMS above 15%; the model and rating at these stations are provisional.

VES	Curve	n. layers	ρ (Ω·m)	h (m)	D (m)	Aquifer ρ (Ω·m)	Aquifer h (m)	Aquifer D (m)	RMS (%)	GWP
VES 1	A	3	48.9 / 115.0 / 513.1	0.7 / 17.6	0.7 / 18.3	115.0	17.6	18.3	7.2	Very Good
VES 2†	H	3	128.5 / 40.9 / 163.7	1.1 / 0.9	1.1 / 2.0	40.9	0.9	2.0	25.1	Moderate
VES 3	HA	4	38.8 / 23.8 / 298.4 / 342.3	2.3 / 2.8 / 3.1	2.3 / 5.1 / 8.2	298.4	3.1	8.2	9.8	Poor
VES 4	H	3	70.7 / 14.3 / 322.2	1.4 / 2.7	1.4 / 4.1	14.3	2.7	4.1	10.6	Moderate
VES 5	H	3	44.7 / 9.3 / 843.4	1.7 / 2.2	1.7 / 3.9	9.3	2.2	3.9	14.3	Moderate
VES 6	A	3	12.4 / 31.5 / 2615.6	0.3 / 8.1	0.3 / 8.4	31.5	8.1	8.4	11.5	Good
VES 7	KH	4	53.3 / 72.6 / 8.7 / 2972.7	1.8 / 0.8 / 3.9	1.8 / 2.6 / 6.5	8.7	3.9	6.5	11.8	Moderate
VES 8†	HK	4	947.1 / 73.1 / 590.8 / 184.2	1.2 / 1.4 / 4.4	1.2 / 2.6 / 7.0	590.8	4.4	7.0	16.2	Poor
VES 9†	H	3	61.3 / 23.9 / 3341.6	0.6 / 10.2	0.6 / 10.8	23.9	10.2	10.8	17.2	Very Good
VES 10	A	3	188.3 / 327.7 / 498.7	4.2 / 20.7	4.2 / 24.9	327.7	20.7	24.9	5.1	Poor
VES 11	H	3	243.0 / 28.2 / 457.9	0.9 / 2.8	0.9 / 3.7	28.2	2.8	3.7	9.9*	Moderate
VES 12	K	3	15.6 / 3712.5 / 3334.7	2.9 / 34.6	2.9 / 37.4	3712.5	34.6	37.4	6.3*	Poor
VES 13	H	3	169.5 / 22.1 / 402.0	0.4 / 3.0	0.4 / 3.5	22.1	3.0	3.5	9.5*	Good
VES 14	H	3	908.0 / 20.8 / 1001.3	0.3 / 12.6	0.3 / 12.9	20.8	12.6	12.9	12.3*	Very Good

VES 15†	H	3	216.9 / 11.5 / 531.4	0.6 / 2.7	0.6 / 3.3	11.5	2.7	3.3	34.0*	Moderate
VES 16	H	3	23.2 / 6.2 / 513.5	1.0 / 1.9	1.0 / 3.0	6.2	1.9	3.0	11.1*	Moderate
VES 17	H	3	459.0 / 22.3 / 735.8	0.8 / 9.0	0.8 / 9.7	22.3	9.0	9.7	10.3*	Good
VES 18†	H	3	1269.2 / 10.6 / 919.2	0.5 / 13.7	0.5 / 14.2	10.6	13.7	14.2	18.3*	Very Good
VES 19†	HA	4	464.3 / 19.6 / 47.0 / 1089.0	1.4 / 2.5 / 23.5	1.4 / 4.0 / 27.5	47.0	23.5	27.5	26.9*	Very Good
VES 20†	KH	4	7.0 / 961.5 / 32.0 / 780.5	0.3 / 1.3 / 5.8	0.3 / 1.6 / 7.4	32.0	5.8	7.4	46.6*	Good

Dar-Zarrouk Parameters and Aquifer Protective Capacity

Table 3 presents the Dar-Zarrouk parameters for the total weathered overburden above fresh basement (H, S, T, ρL, ρT and λ), together with the longitudinal conductance of the protective cover alone (Sc) and the resulting protective-capacity class. The total-overburden conductance S ranges from 0.028 mho (VES 8) to 1.293 mho (VES 18), but it includes the conductive weathered-basement horizon that constitutes the aquifer itself and therefore does not measure the protection afforded to that aquifer. At VES 18, for example, S is dominated by the 13.7 m weathered horizon of 10.6 Ω·m, whereas the overlying 0.5 m cover has a resistivity of 1269.2 Ω·m. Using Sc, which excludes the aquifer horizon, conductance ranges from below 0.001 mho (VES 14 and 18) to 0.186 mho (VES 12): seventeen stations fall in the poor class (Sc < 0.1 mho) and three (VES 3, 12 and 19) in the weak class (0.1–0.19 mho); no station reaches the moderate or higher classes. A thin and generally resistive cover, consistent with a thin sandy-lateritic weathering profile, therefore provides little electrical evidence of natural protection across the survey area. This is in line with the generally low conductance values reported for Guyuk (S = 0.001–0.87 mho; Usman Baba et al., 2026) and Asaba (S = 0.011–0.124 mho; Chukwusa et al., 2026), although the intervals used in those studies may differ, so the comparison is only indicative.

Protective capacity and prospectivity do not coincide. Of the four stations rated poor for geoelectric prospectivity, VES 3 and VES 12 have the highest cover conductance in the survey (Sc = 0.177 and 0.186 mho), whereas VES 8 and VES 10 have Sc of 0.020 and 0.022 mho. Conversely, VES 14 and VES 18 combine a very good prospectivity rating with Sc below 0.001 mho, because a thin, highly resistive topsoil (908.0 and 1269.2 Ω·m, respectively) overlies the weathered aquifer; such a cover implies little clay to retard infiltration and is not evidence of a well-protected aquifer. VES 19, which has the thickest overburden (27.4 m) among the very-good stations, has the largest Sc of those stations (0.131 mho) but is still weak and its model is marginal (RMS 26.9%). At VES 12, the transverse resistance of the total overburden (T ≈ 128,498 Ω·m²) and the coefficient of anisotropy (λ = 4.22) are the highest in the dataset, reflecting the very high resistivity contrast between its thin, conductive topsoil and its exceptionally resistive intermediate layer. Sc is also the least certain parameter: the cover at VES 6, 13, 14, 18 and 20 is only 0.3–0.5 m thick, which is less than the smallest electrode spacing (AB/2 = 1 m), so its thickness and resistivity are poorly resolved and the corresponding Sc values should be treated as approximate. The low cover conductance is consistent with, though not validated by, the heavy bacteriological contamination reported for shallow hand-dug wells in Lapai (mean E. coli 65.50 cfu/100 mL; Amadi et al., 2017). That contamination can also arise from direct entry through uncovered or poorly sealed wells and from nearby soakaways, so it does not test the protective-capacity classes. Completed boreholes at any station should incorporate sanitary wellhead protection (grouted casing, concrete apron, adequate offset from latrines and waste pits), and the protective-capacity classes should not be equated with confirmed contaminant attenuation.

Table 3: Dar-Zarrouk parameters for all twenty VES stations. H = total thickness of the weathered overburden above fresh basement; S = its longitudinal unit conductance; T = transverse unit resistance; ρL and ρT = average longitudinal and transverse resistivities; λ = coefficient of anisotropy. Sc = longitudinal conductance of the protective cover only (layers above the top of the inferred aquifer), on which the protective-capacity class is based (empirical scheme after Henriet, 1976, as applied in Nigerian basement studies; see text). † = RMS misfit above 15% (Table 2); values are provisional.

VES	H (m)	S (mho)	T (Ω·m²)	ρL (Ω·m)	ρT (Ω·m)	Λ	S_c (mho)	Protective Capacity
VES 1	18.3	0.167	2058.2	109.3	112.5	1.01	0.014	Poor
VES 2†	2.0	0.031	178.2	65.4	89.1	1.17	0.009	Poor
VES 3	8.2	0.187	1080.9	43.8	131.8	1.74	0.177	Weak
VES 4	4.1	0.209	137.6	19.7	33.6	1.31	0.020	Poor
VES 5	3.9	0.275	96.5	14.2	24.7	1.32	0.038	Poor
VES 6	8.4	0.281	258.9	29.9	30.8	1.02	0.024	Poor
VES 7	6.5	0.493	187.9	13.2	28.9	1.48	0.045	Poor
VES 8†	7.0	0.028	3838.4	251.2	548.3	1.48	0.020	Poor
VES 9†	10.8	0.437	280.6	24.7	26.0	1.02	0.010	Poor
VES 10	24.9	0.086	7574.2	291.3	304.2	1.02	0.022	Poor
VES 11	3.7	0.103	297.7	35.9	80.4	1.50	0.004	Poor
VES 12	37.5	0.195	128497.7	192.1	3426.6	4.22	0.186	Weak
VES 13	3.4	0.138	134.1	24.6	39.4	1.27	0.002	Poor
VES 14	12.9	0.606	534.5	21.3	41.4	1.40	<0.001	Poor
VES 15†	3.3	0.237	161.2	13.9	48.8	1.88	0.003	Poor
VES 16	2.9	0.350	35.0	8.3	12.1	1.21	0.043	Poor
VES 17	9.8	0.405	567.9	24.2	57.9	1.55	0.002	Poor
VES 18†	14.2	1.293	779.8	11.0	54.9	2.24	<0.001	Poor
VES 19†	27.4	0.631	1803.5	43.5	65.8	1.23	0.131	Weak
VES 20†	7.4	0.226	1437.7	32.8	194.3	2.43	0.044	Poor

General Discussion

The geoelectric framework established here is broadly consistent with the regional basement-complex setting reported for Lapai and comparable parts of Niger State (Ndanusa et al., 2026; Obiora & Ibuot, 2018; Batagarawa & Onoduku, 2014). The quantitative comparison with the earlier twelve-station Lapai survey is presented in the following paragraph. The dominance of H- and A-type curves (fourteen of twenty stations) indicates a weathered horizon between a resistive cover and the fresh basement at most stations, while the K-, HK- and KH-type responses (VES 12, 8, 7 and 20) and the HA-type response at VES 3 flag localised zones where a resistive horizon occupies or overlies the weathered-basement position and may reduce the productivity of the shallow aquifer. The resistive horizons at VES 3, 8, 10 and 12 account for their poor prospectivity ratings, whereas the conductance of the protective cover is controlled mainly by the thin topsoil, so that prospectivity and protective capacity vary largely independently.

A quantitative comparison with the earlier Lapai survey (Ndanusa et al., 2026) shows that the Maraban Lapai weathered profile is thinner. At the 16 stations where the weathered-basement horizon is not markedly resistive, its resistivity (6.2–115 Ω·m, median 22 Ω·m) lies within the 11–140 Ω·m reported for the twelve-station survey. However, the median modelled thickness of the weathered horizon across all twenty stations is 5.1 m (range 0.9–34.6 m), against 12–22 m earlier, and the median depth to its base is 7.8 m (range 2.0–37.4 m), against 14–22.5 m; only five of the twenty stations reach 14 m, and the single station deeper than 34 m (VES 12) is the resistive K-type site. The topsoil layer is also thinner here (median 0.95 m, range 0.3–4.2 m) than the 2.0–4.0 m listed in the earlier survey's Table 2. Regional borehole lithology places the productive aquifer in basement Lapai at 34–40 m (Bashir et al., 2014), deeper than the modelled base of the weathered horizon at nearly all present stations, so productive zones may lie in fractured basement beneath the weathered layer, which these soundings do not resolve. The regional compilation of Idris-Nda et al. (2015) reports weathering depths of 2–30 m and fracture depths of 25–130 m across the Niger State basement, with borehole depths of 30–200 m (mean about 50 m). The modelled base of the weathered horizon here (2.0–27.5 m at all stations except VES 12, at 37.4 m) falls within the weathering range, whereas the reported fracture depths and typical borehole depths lie below it. Because Lapai is also a basement–sedimentary contact area with reportedly poor and deep boreholes, lateral changes in lithology over short distances may violate the horizontal-layering assumption of the one-dimensional soundings and may

partly explain the low yields reported for such areas; this should be tested with two-dimensional imaging and borehole records. The principal joint direction in Lapai is reported as NE–SW, conforming to the regional fracture trend (Amadi et al., 2017), so any fracture control on deeper yields would be aligned in that direction, which one-dimensional soundings cannot resolve. These comparisons are between interpreted models from different surveys, and not between ground-truthed hydrogeological measurements.

A borehole sited without geophysical control at VES 3, 8, 10 or 12 might encounter a compact, poorly saturated horizon and yield little water; geophysical screening of the kind reported here can reduce, but not eliminate, this risk (Olayinka, 1996). The five very-good stations (VES 1, 9, 14, 18 and 19) are spread across the northern and eastern portions of the survey area rather than concentrated in a single cluster, which suggests that the weathered aquifer, where present, is not laterally continuous across Maraban Lapai but may occur in discrete pockets; this inference rests on the station spacing and should be tested with two-dimensional imaging. Alternative geological interpretations are also possible. A high-resistivity layer at the weathered-basement position could represent dry weathered material, ferruginised laterite or resistive saprock, and a low-resistivity layer may reflect clay-rich regolith rather than a productive aquifer, so low resistivity alone is not evidence of high yield. The quality of the inversion fits bears directly on the practical recommendations: three of the five very-good stations (VES 9, 18 and 19) and VES 20 (good) have RMS misfit above 15%, and their ratings, depths and thicknesses may change when their models are verified.

As with any VES-based investigation, the results presented here carry inherent limitations. The one-dimensional Schlumberger technique is non-unique (equivalent models can fit the same data), assumes horizontal layering beneath each sounding centre and cannot resolve lateral geological discontinuities that fall within the inter-station spacing; the RMS misfit above 15% recorded at seven stations (Table 2) further indicates that the layer parameters at these stations should be treated with greater caution than at the lower-misfit soundings. Layers thinner than the first electrode spacing are poorly resolved, and the deepest (basement) resistivities are constrained only by the last few readings at AB/2 = 100 m. None of the interpreted models has yet been ground-truthed against borehole lithological logs or pumping-test data, and no hydrochemical analysis has been carried out, so groundwater quality at the identified prospects remains uncharacterised. Complementary two-dimensional resistivity imaging, hydrochemical sampling and, ultimately, pilot borehole drilling at the very-good and good-prospectivity stations are recommended to validate and extend the present findings.

CONCLUSION

This study applied the Schlumberger vertical electrical sounding technique, combined with Dar-Zarrouk parameter analysis, at twenty stations around Maraban Lapai, Niger State, to give a preliminary geoelectric characterisation of the basement complex aquifer system. Three- and four-layer resistivity models resolve eleven H-type, three A-type, two HA-type, two KH-type, one HK-type and one K-type sounding curves. The inferred weathered-basement horizon has its base at depths of 2.0–37.4 m, with resistivity ranging from 6.2 to 3,712.5 Ω·m. On resistivity and modelled thickness, five stations (VES 1, 9, 14, 18 and 19) are classed as very good and four (VES 6, 13, 17 and 20) as good geoelectric prospects. These stations are proposed as candidate targets for further investigation and not as confirmed groundwater-development locations; VES 9, 18 and 19 (very good) and VES 20 (good) have RMS misfit above 15%, so their ratings are provisional until the models are verified. When only the layers above the inferred aquifer are considered, the cover has low longitudinal conductance at every station (Sc from below 0.001 to 0.186 mho; seventeen stations poor and three weak), which indicates little electrical evidence of natural protection of the aquifer. Boreholes in the area should therefore incorporate sanitary wellhead protection. Drilling depths should be set station by station from the modelled base of the weathered horizon (about 3.5–27.5 m at these stations); penetration of the underlying basement would depend on fractures that one-dimensional soundings do not resolve. None of these inferences has yet been validated against borehole logs, water-table observations or pumping tests.

This work extends the geoelectric baseline previously established for the Lapai basement complex (Ndanusa et al., 2026) to Maraban Lapai specifically and adds a protective-capacity analysis that was absent from that earlier survey. It offers a preliminary, station-by-station guide to where further hydrogeological work is most justified. Repeat soundings at the high-misfit stations, two-dimensional electrical resistivity tomography, hydrochemical profiling, pilot boreholes with lithological logging and pumping tests are needed to validate the findings before they are used for borehole development.

Acknowledgement

The authors acknowledge the cooperation of the community leaders and landowners of Maraban Lapai who facilitated access to the measurement stations during field data acquisition.

REFERENCES

Amadi, A. N., Olasehinde, P. I., Obaje, N. G., Unuevho, C. I., Yunusa, M. B., Keke, U. N., & Ameh, I. M. (2017). Investigating the quality of groundwater from hand-dug wells in Lapai, Niger State using physico-chemical and bacteriological parameters. Minna Journal of Geosciences, 1(1), 77–92.

Barker, R. D. (1989). Depth of investigation of collinear symmetrical four-electrode arrays. Geophysics, 54(8), 1031–1037. https://doi.org/10.1190/1.1442738

Bashir, I. Y., Izham, M. Y., & Main, R. (2014). Vertical electrical sounding investigation of aquifer composition and its potential to yield groundwater in some selected towns in Bida Basin of North Central Nigeria. Journal of Geography and Geology, 6(1), 60–69. https://doi.org/10.5539/jgg.v6n1p60

Batagarawa, S. M., & Onoduku, U. S. (2014). Evaluation of groundwater potential of parts of the basement complex of Minna area, Niger State, using resistivity method. Journal of Environment and Earth Science, 4(2), 17–28.

Chukwusa, F. O., Onifade, Y. S., Olaseni, V. B., & Eyankware, M. O. (2026). Application of geoelectric and hydrogeological methods in delineation of aquifer potential and protective capacity in parts of Asaba Metropolis, Niger Delta region of Nigeria. Nigerian Journal of Physics, 35(4), 220–235. https://doi.org/10.62292/njp.v35i4.2026.673

Dada, S. S. (2006). Proterozoic evolution of Nigeria. In O. Oshi (Ed.), The basement complex of Nigeria and its mineral resources (pp. 29–44). Akin Jinad and Co.

Henriet, J. P. (1976). Direct application of the Dar Zarrouk parameters in ground water surveys. Geophysical Prospecting, 24(2), 344–353. https://doi.org/10.1111/j.1365-2478.1976.tb00931.x

Idris-Nda, A., Abubakar, S. I., Waziri, S. H., Dadi, M. I., & Jimada, A. M. (2015). Groundwater development in a mixed geological terrain: A case study of Niger State, central Nigeria. WIT Transactions on Ecology and the Environment, 196, 77–87. https://doi.org/10.2495/WRM150071

Jones, H. A., & Hockey, R. D. (1964). The geology of part of south-western Nigeria (Bulletin No. 31). Federal Government Printer.

Kearey, P., Brooks, M., & Hill, I. (2002). An introduction to geophysical exploration (3rd ed.). Blackwell Science.

Koefoed, O. (1979). Geosounding principles, 1: Resistivity sounding measurements. Elsevier.

Maillet, R. (1947). The fundamental equations of electrical prospecting. Geophysics, 12(4), 529–556. https://doi.org/10.1190/1.1437342

Ndanusa, H. H., Aweda, A. K., Tanko, Y. U., Yabagi, J. A., & Saleh, A. (2026). Deployment of electrical resistivity method for evaluation of sustainable groundwater resources in Lapai, Niger State, Nigeria. Nigerian Journal of Physics, 35(4), 310–317. https://doi.org/10.62292/njp.v35i4.2026.695

Obiora, D. N., & Ibuot, J. C. (2018). Hydrogeophysical evaluation of aquifer characteristics and groundwater potential in Minna, Niger State, Nigeria. Geosciences, 8(2), 46. https://doi.org/10.3390/geosciences8020046

Olayinka, A. I. (1996). Geophysical siting of boreholes in crystalline basement areas of Africa. Journal of African Earth Sciences, 22(4), 585–592. https://doi.org/10.1016/0899-5362(96)00035-2

Olayinka, A. I., & Yaramanci, U. (2000). Assessment of the reliability and limitations of 2-D resistivity imaging for groundwater exploration in crystalline rocks. Journal of Applied Geophysics, 45(1), 1–16. https://doi.org/10.1016/S0926-9851(00)00016-2

Olorunfemi, M. O., & Fasuyi, S. A. (1993). Aquifer types and the geoelectric/hydrogeologic characteristics of part of the central basement terrain of Nigeria (Niger State). Journal of African Earth Sciences, 16(3), 309–317. https://doi.org/10.1016/0899-5362(93)90051-Q

Oniku, A. S., Sunu, S. A., Nur, A., Timtere, P., & Kenda, L. P. (2025). Integrated GIS technique and electrical resistivity sounding (ERS) for groundwater prospecting in Yola catchment area, Northern Upper Benue Trough, Nigeria. Nigerian Journal of Physics, 34(2), 108–123 https://doi.org/10.62292/njp.v34i2.2025.376

Orellana, E., & Mooney, H. M. (1966). Master tables and curves for vertical electrical sounding over layered structures. Interciencia.

Osumeje, J. O., Eshimiakhe, D., Oniku, A. S., & Lawal, K. M. (2024). Application of remote sensing and electrical resistivity technique for delineating groundwater potential in North Western Nigeria.

Scientific Reports, 14(1), 22299. https://doi.org/10.1038/s41598-024-69633-8

Rahaman, M. A. (1976). Review of the basement geology of south-western Nigeria. In C. A. Kogbe (Ed.), Geology of Nigeria (pp. 41–58). Elizabethan Publishing.

Telford, W. M., Geldart, L. P., & Sheriff, R. E. (1990). Applied geophysics (2nd ed.). Cambridge University Press.

Usman Baba, A., Ahmed, N., & Sulaiman, A. (2026). Evaluation of groundwater potential using vertical electrical sounding and Dar Zarouk parameters in Guyuk and its environs, Northeastern Nigeria. Nigerian Journal of Physics, 35(3), 247–257. https://doi.org/10.62292/njp.v35i3.2026.608

Vander Velpen, B. P. A. (1988). RESIST version 1.0: A computer program for the processing and interpretation of resistivity sounding data (M.Sc. research project). International Institute for Aerospace Survey and Earth Sciences (ITC), Delft, The Netherlands.

Vander Velpen, B. P. A., & Sporry, R. J. (1993). RESIST: A computer program to process resistivity sounding data on PC compatibles. Computers & Geosciences, 19, 691–703.